

Rotational spectroscopy of isotopic vinyl cyanide, $\text{H}_2\text{C}=\text{CH}-\text{C}\equiv\text{N}$, in the laboratory and in space^{*}

Holger S.P. Müller^{a,b,*}, Arnaud Belloche^b, Karl M. Menten^b,
Claudia Comito^b, Peter Schilke^b,

^a*I. Physikalisches Institut, Universität zu Köln, Zùlpicher Str. 77, 50937 Köln, Germany*

^b*Max-Planck Institut für Radioastronomie, Auf dem Hügel 69, 53121 Bonn, Germany*

Abstract

The rotational spectra of singly substituted ^{13}C and ^{15}N isotopic species of vinyl cyanide have been studied in natural abundances between 64 and 351 GHz. In combination with previous results, greatly improved spectroscopic parameters have been obtained which in turn helped to identify transitions of the ^{13}C species for the first time in space through a molecular line survey of the extremely line-rich interstellar source Sagittarius B2(N) in the 3 mm region with some additional observations at 2 mm. The ^{13}C species are detected in two compact ($\sim 2.3''$), hot (170 K) cores with a column density of $\sim 3.8 \times 10^{16}$ and $1.1 \times 10^{16} \text{ cm}^{-2}$, respectively. In the main source, the so-called “Large Molecule Heimat”, we derive an abundance of 2.9×10^{-9} for each ^{13}C species relative to H_2 . An isotopic ratio $^{12}\text{C}/^{13}\text{C}$ of 21 has been measured. Based on a comparison to the column densities measured for the ^{13}C species of ethyl cyanide also detected in this survey, it is suggested that the two hot cores of Sgr B2(N) are in different evolutionary stages. Supplementary laboratory data for the main isotopic species recorded between 92 and 342 GHz permitted an improvement of its spectroscopic parameters as well.

Key words: vinyl cyanide, acrylonitrile, propenenitrile, rotational spectroscopy, submillimeter wave spectroscopy, interstellar molecule, star-forming region, Sagittarius B2

^{*} This work is dedicated to Edward A. Cohen and Herbert M. Pickett in recognition of their many contributions to the theory and application of molecular spectroscopy.

^{*} Corresponding author.

Email addresses: hspm@ph1.uni-koeln.de (Holger S.P. Müller),

1 Introduction

Vinyl cyanide, (VyCN for short), also known as acrylonitrile or propenenitrile, $\text{H}_2\text{C}=\text{CH}-\text{C}\equiv\text{N}$ or shorter $\text{C}_2\text{H}_3\text{CN}$, is an important molecule in space. It was detected in the massive star-forming region Sagittarius B2 (Sgr B2 for short) by Gardner and Winnewisser as early as 1975 [1]. Massive star-forming regions are comparatively dense and hot, thus, transitions of VyCN in its $v_{11} = 1$ and $v_{15} = 1$ excited vibrational states have been detected in Orion KL [2] and in Sgr B2(N) [3]. Matthews and Sears reported the first detection of this molecule in a dark cloud (TMC-1) [4]; and very recently, Agúndez et al. reported its detection in the circumstellar envelope of the late-type star IRC +10216 (CW Leo) [5].

VyCN had also been among the molecules whose rotational spectra were studied rather early by Wilcox et al. in 1954 [6] and by Costain and Stoicheff in 1959 [7]. The latter also investigated the singly-substituted ^{13}C species as well as $\text{C}_2\text{H}_3^{15}\text{N}$ and H_2CCDCN . More recently, additional reports have been published [8,9,10,11,12,13,14]. Its dipole moment components [6,10] as well as increasingly accurate ^{14}N hyperfine structure parameters [7,10,13,14] have been obtained. A total of 14 isotopic species have been investigated in Ref [14], including all stable singly substituted ones, all multiply deuterated ones except D_2CCHCN , and the singly substituted ^{13}C species of H_2CCDCN . The rotational constants were used to derive structural parameters according to several structural models. Finally, a combined fit of these previous data was reported by Thorwirth et al. in their work on the related vinyl acetylene molecule [15].

We have carried out millimeter line observations of Sgr B2(N) with the IRAM 30 m telescope. These observations yielded a variety of interesting results, e.g. the first detection of aminoacetonitrile, a possible precursor of the simplest aminoacide glycine, which was secured by accompanying interferometric observations [16]. In the course of the ongoing analyses of the observational data supplementary laboratory spectroscopic investigations have been carried out to facilitate these and future analyses.

In the present contribution we report on laboratory rotational spectroscopic investigations of the singly substituted isotopic species of VyCN containing ^{13}C or ^{15}N as well as supplementary data on the main isotopic species. In addition, we present the first detection of ^{13}C containing isotopologues of VyCN in space.

`belloche@mpifr-bonn.mpg.de` (Arnaud Belloche), `menten@mpifr-bonn.mpg.de` (Karl M. Menten), `ccomito@mpifr-bonn.mpg.de` (Claudia Comito), `schilke@mpifr-bonn.mpg.de` (Peter Schilke).

2 Experimental details

Conventional absorption spectroscopy was employed in Cologne for the laboratory investigations. The measurements were carried out in a 3 m long glass cell at room temperature in a static mode. A commercial $\text{C}_2\text{H}_3\text{CN}$ sample was used at pressures of less than 1 Pa for stronger lines and around 2 Pa for the generally weak lines. Two commercial millimeter-wave synthesizers AM-MSP 1 and 2 (Analytik & Meßtechnik GmbH, Chemnitz, Germany) covered the 4 and 3 mm frequency ranges (52–119 GHz); because of the detector cut-off, the lowest measured line was near 64 GHz. Additional measurements have been performed in the frequency range 239–351 GHz with the Cologne Terahertz Spectrometer [17] using a phase-locked backward-wave oscillator as source. A liquid He-cooled InSb hot-electron bolometer was used as detector throughout the investigations.

The uncertainties of the lines were estimated by judging the line shape and the signal-to-noise ratios. Investigations, e. g., into rotational spectra of SO_2 [18] and SiS [19] demonstrated that relative uncertainties $\Delta\nu/\nu$ of 10^{-8} and better can be achieved up to and even beyond 1 THz in our laboratory not only for strong, but also for fairly weak, isolated lines.

3 Observed laboratory spectra and analysis

Vinyl cyanide is a planar asymmetric top that is, with $\kappa = -0.9798$ for the main isotopic species in its ground vibrational state, quite close to the prolate symmetric limit of -1 . It has a large a -dipole moment component of 3.815 (12) D and a considerably smaller, but still sizeable b -dipole moment component of 0.894 (68) D [10]. The ^{14}N hyperfine splitting can be resolved easily at low values of J [10,14]. It can be resolved at least in part for higher- J values in a -type R -branch transitions when K_a approaches J [13], see also Fig. 1. In this context, it is interesting to note that Gerry and Winnemisser [8] published two candidate lines for the $J = 14 - 13$, $K_a = 13$ transition at 133180.473 and 133181.018 MHz. In fact, both lines belong to this transition; the former is the $F = J$ hyperfine component, whereas the latter is the overlap of the $F = J \pm 1$ hyperfine components. In those days, ~ 35 years ago, it was probably neither expected nor feasible to calculate hyperfine splitting at such comparatively high quantum numbers.

Selected a -type R -branch transitions of the singly substituted ^{13}C and ^{15}N isotopic species of VyCN were readily found in the 4 and 3 mm regions based on the previous data. ^{14}N hyperfine splitting was resolved in part for transitions with high K_a values as shown in Fig. 1. Subsequently, selected transitions

were searched for at 239 – 253 GHz, around 320 GHz, and near 350 GHz. No *b*-type transitions were searched for specifically at lower frequencies as these were not only weak, but also their uncertainties were comparatively large initially. Nevertheless, some *b*-type transitions could be identified for all the ^{13}C -containing species in wider scans around the *a*-type *R*-branch transitions of the main isotopic species recorded in the 4 and 3 mm regions. The measurements at higher frequencies improved the predictions for these assignments. Moreover, one $K_a = 1 - 0$ transition each was found for $\text{H}_2\text{C}^{13}\text{CHCN}$ and for $\text{H}_2\text{CCH}^{13}\text{CN}$ near 245 and 250 GHz, respectively. One should keep in mind that even though the *b*-type transitions of these isotopic species are considerably stronger at these higher frequencies, those of the main isotopic species in the molecule’s ground and low-lying excited states are stronger, too. Moreover, the number of *a*-type *R*-branch transitions increases with J . Overall, this results in a strongly increased probability for overlap of two lines or for perturbations of the apparent line positions caused by the proximity of two lines as can be seen in Fig. 2.

The maximum J values were 35 to 38 for the minor isotopic species, and the K_a values reached 17 to 20.

Selected transitions were recorded for the main isotopic species in similar frequency regions. The transitions were easily found because of the extensive data set from previous laboratory studies [8,9,10,11,12,13,14]. The maximum J and K_a values were 80 and 30, respectively.

The data obtained in the course of the present investigation were fit together with previous data. Uncertainties of 100 kHz were given for the microwave transitions from Refs. [8,9] as stated in the former. Average frequencies were used for the few lines that were reported in both studies, and the uncertainties were set to 70 kHz. Millimeter-wave transitions from [8] quoted to 10 kHz digits were given 150 kHz uncertainties as stated; those quoted to 1 kHz digits were reported to be more accurate by more than a factor of 10, suggesting uncertainties of 10 kHz. While this seemed to be reasonable for essentially all transitions not affected by partially resolved hyperfine structure, 20 kHz appeared to be more appropriate for those that were affected. The reported uncertainties were largely used for the experimental lines from Refs. [10,12,14]; 50 and 5 kHz, respectively, were ascribed to the data from Refs. [11,13] on the basis of the average residuals between observed and calculated frequencies in these two papers. Very few transitions were omitted from the final fits because of large residuals. These included the weak $F = 1 - 0$ hyperfine components of the $J_{K_a,K_c} = 2_{1,2} - 1_{1,1}$ transition for $\text{H}_2^{13}\text{CCHCN}$ and $\text{H}_2\text{C}^{13}\text{CHCN}$ [14] because trial fits with these lines weighted out not only increased the residuals of these two lines by a factor of about two but also improved the quality of the fit.

The spectroscopic parameters determined for the main isotopic species are essentially the same as in Ref. [15]. Two additional decic and one dodecic parameters were necessary to fit the high- K_a a -type R -branch transitions. Initial parameters for the minor isotopic species were taken from Ref. [14] and transformed to Watson’s S -reduction. Higher order parameters were taken from the main isotopic species and scaled by the appropriate powers of the ratios of $2A - B - C$, $B + C$, and $B - C$. As observed previously [14], D_K did not follow this trend. Thus, H_K and L_K were derived similarly from the ratios of D_K . The resulting spectroscopic parameters are given in Table 1.

The experimental transition frequencies with assignments and uncertainties as well as residuals between observed frequency and those calculated from the final set of spectroscopic parameters are available as supplementary material (Table S1). The detailed fit files as well as related files will be available in the Cologne Database for Molecular Spectroscopy, CDMS¹ [21,22], as will be extensive predictions of the rotational spectra.

4 Radioastronomical observations

We carried out a complete line survey in the 3 mm atmospheric window between 80 and 116 GHz toward the hot core region Sagittarius B2(N) (hereafter Sgr B2(N) for short). Additional spectra were also obtained in the 2 and 1.3 mm windows. The observations were performed in January 2004, September 2004, and January 2005 with the IRAM 30m telescope on Pico Veleta, Spain. Details about the observational setup and the data reduction are given in [16]. An rms noise level of 15–20 mK on the T_a^* scale was achieved below 100 GHz, 20–30 mK between 100 and 114.5 GHz, and about 50 mK between 114.5 and 116 GHz.

The overall goal of our survey was to characterize the molecular content of Sgr B2(N). It also allows searches for new species once all the lines emitted by known molecules have been identified, including vibrationally and torsionally excited states. We detected about 3700 lines above 3σ over the whole 3 mm band. These numbers correspond to an average line density of about 100 features per GHz. Given this high line density, the assignment of a line to a given molecule can be trusted only if all lines emitted by this molecule in our frequency coverage are detected with the right intensity and no predicted line is missing in the observed spectrum. The XCLASS software (see [25]) was used to model the emission of all known molecules in the local thermodynamical equilibrium approximation (LTE for short). More details about this analysis are given in [16]. So far, we have identified 51 different molecules, 60

¹ <http://www.astro.uni-koeln.de/vorhersagen/>; short-cut: <http://www.cdms.de/>

isotopologues, and 41 vibrationally/torsionally excited states in Sgr B2(N). This represents about 60% of the lines detected above the 3σ level.

The frequency ranges covered at 3 and 2 mm contain several hundred transitions of the three ^{13}C isotopologues of VyCN. The LTE modeling shows, however, that the transitions with the line strength times the appropriate dipole moment, $S\mu^2$, smaller than 40 D^2 are much too weak to be detectable with the sensitivity we achieved and the physical parameters we explored. Out of 291 transitions above this $S\mu^2$ threshold, 194 are detected in our line survey toward Sgr B2(N), either well isolated or in groups, or somewhat blended with emission from other molecules. The remaining 97 transitions are heavily blended with emission from other molecules or weaker than the noise level, and cannot be identified in our spectrum. The detected transitions are listed in Table S2 of the supplementary material. To save some space, when two transitions have a frequency difference smaller than 0.1 MHz which is not resolved in our astronomical data, only the first one is listed. The transitions are numbered in Col. 1, and their quantum numbers are given in Col. 3. The identities of the ^{13}C isotopologues are coded in Col. 2. The frequencies, the frequency uncertainties, the energies of the lower levels in temperature units, and the $S\mu^2$ values are listed in Col. 4, 5, 6, and 7, respectively. Since the spectra are in most cases close to the line confusion limit and it is difficult to measure the noise level, we give in Col. 8 the rms sensitivity computed from the system temperature and the integration time (see [16] for details). The isolated transitions or groups of transitions that could be easily identified are labeled “no blend” in Col. 13, while for the other transitions we indicate which molecule contaminates the observed line. We identified the lines of the ^{13}C isotopologues of VyCN and the blends affecting them with the LTE model of these three molecules and the LTE model including all molecules identified in our survey thus far. Table 2 shows the parameters of our best-fit LTE model of the ^{13}C isotopologues of VyCN as well as the parameters of our best-fit LTE model of VyCN itself.

The detected transitions are grouped into “features” as listed in Col. 9 of Table S2 of the supplementary material, a feature being an observed line containing one or more (overlapping) transitions of the ^{13}C isotopologues of VyCN. There are 89 features detected toward Sgr B2(N), 10 of which look relatively free of contamination and an additional 16 are only slightly blended with emission from other molecules. The remaining 63 features are blended with emission from other molecules but with the ^{13}C isotopologues of VyCN contributing significantly (at least $\sim 50\%$) to the peak intensity according to our LTE modeling. The integrated intensities of all detected features are given in Col. 10, along with the integrated intensities of our best-fit model of the ^{13}C isotopologues of VyCN (Col. 11) and of the best-fit model including all molecules (Col. 12). Two selected frequency ranges containing Features F12 to F19 and F32 to F37 are shown in Fig. 3. The synthesized spectrum

corresponding to the three ^{13}C isotopologues of VyCN is plotted in red, while the model including all molecules is overlaid in green.

We derived the model parameters shown in Table 2 from all the constraints provided by the transitions of the ^{13}C isotopologues but also from the main isotopic species which we easily detect in our survey in the ground state and in several vibrationally excited states (Belloche et al., *in prep.*, see also [3]). The strongest velocity component is detected at 63 km s^{-1} and corresponds to the so-called “Large Molecule Heimat” (see [16]). The second velocity component at 73 km s^{-1} is weaker, but still obvious in many transitions of the main isotopologue in the ground state and in the $v_{11} = 1$ and $v_{15} = 1$ vibrationally excited states. It is also detected in many transitions of the ^{13}C isotopologues (e.g. in Feature 16 of Fig. 3). The third (wing) component at 55 km s^{-1} is much weaker. It is well seen in many transitions of the main isotopic species of vinyl cyanide and is (barely) detected in Feature 44 of $^{13}\text{CH}_2\text{CHCN}$, but it is too weak to be detected in all other ^{13}C isotopologue transitions covered by our survey. The maximum opacity of the ^{13}C isotopologue transitions is 0.5 in our LTE model. Therefore these transitions are optically thin and the source size and column density are degenerated. On the other hand many transitions of the main isotopic species are optically thick, which allowed to derive the source size, once a good estimate of the temperature had been obtained. The same source size was used for all ^{13}C isotopologues. Finally, no attempts were made to fit the transitions in the 1.3 mm window since the line confusion is much more severe and the position of the baselines much more uncertain. In addition, our LTE model predicts emission line intensities stronger than observed for many molecules in this window. Apart from the uncertain baselines, the level of which is likely to be overestimated because of line confusion, we suspect that the dust emission is optically thick in this window and affects significantly the line emission from the compact hot cores, but we have not tried to model this effect so far.

Finally, we searched for $\text{C}_2\text{H}_3\text{C}^{15}\text{N}$ in our survey toward Sgr B2(N) but did not detect this isotopologue. Using the same source size, temperature, and linewidth as for the ^{13}C isotopologues, a column-density upper limit of $3 \times 10^{15} \text{ cm}^{-2}$ could be derived in the LTE approximation. From a tentative detection of the ^{15}N isotopologue of cyanoacetylene HC_3N in our survey toward Sgr B2(N) (Belloche et al., *in prep.*), we derive a $^{13}\text{C}^{14}\text{N}/^{12}\text{C}^{15}\text{N}$ ratio of about 15, while Wilson and Rood [27] mention a ratio larger than 30 for the Galactic Center region. In any case, the column-density upper limit derived here for $\text{C}_2\text{H}_3\text{C}^{15}\text{N}$ is consistent with both values.

5 Discussion of laboratory spectroscopic investigations

The hyperfine parameters are largely determined by the data published in Ref. [14]; additional information obtained in the present work for the isotopic species with ^{13}C or previously for the main isotopologue [8,10,13] have very small effects. Omission of one hyperfine component each for $\text{H}_2^{13}\text{CCHCN}$ and $\text{H}_2\text{C}^{13}\text{CHCN}$ actually increased their uncertainties of χ_{bb} and χ_{cc} slightly and changed their values by an amount slightly outside the combined uncertainties.

The mechanical parameters for the main isotopic species agree very well with those determined in a recent combined fit [15]. The uncertainties in the present work are somewhat smaller despite using three additional distortion parameters. These parameters are of the right order of magnitude when compared with the lower order parameters. Three of the off-diagonal octic distortion terms (l_2 , l_3 , and l_4) are barely determined. Nevertheless, they were retained in the final fit as their values seemed to be of the correct order of magnitude. Moreover, omitting any one of these parameters deteriorated the fit slightly and had only modest effects on the remaining parameters. The values of the higher order distortion parameters should be viewed with some caution as additional experimental transition frequencies and the inclusion of still higher order terms may affect their values somewhat outside the reported uncertainties.

Considerably more distortion parameters have been determined for the minor isotopic species in the present work compared with the previous study of Colmont et al. [14]. Because of the change in reduction a direct comparison is not always possible. However, Δ_K and D_K are very similar in a near-prolate top as VycN . Their estimates of the former agree very well with the presently determined D_K value, even in the case of the ^{15}N species for which we did not observe b -type transitions. The distortion parameters of the minor isotopic species are very close to those of the main isotopic species as one would expect because the rotational constants are also quite similar. The use of higher order parameters transferred from the main isotopic species and kept fixed in the analysis may seem excessive at first sight, in particular if one keeps in mind that some of these are comparatively uncertain. However, most of the fits for the minor isotopic species were performed without the parameters higher than those of octic order (the L s). In those fits, the values for L_{KKJ} were much smaller than that of the main isotopic species (by about a factor of 1.5) whereas those for L_{JK} were much larger in magnitude than that of the main isotopic species (by about a factor of 1.5 – 2). With estimates for these high-order parameters included in the fit the values for L_{KKJ} and L_{JK} changed only barely from those of the main isotopologue if the uncertainties are taken into account.

6 Discussion of the radioastronomical detection

We have detected the three ^{13}C isotopologues of vinyl cyanide toward Sgr B2(N). Although many transitions are blended with emission from other molecules, 26 features have been found completely free of contamination or only slightly contaminated. The emission arises from several velocity components. The two velocity components at 63 and 73 km s^{-1} were also detected by Belloche et al. [16] with the IRAM Plateau de Bure interferometer (PdBI) and the Australia Telescope Compact Array (ATCA) in ethyl cyanide $\text{C}_2\text{H}_5\text{CN}$, cyanoacetylene HC_3N and its isotopologue HC^{13}CCN in their $v_7 = 1$ excited states, and methanol CH_3OH in its excited state $v_t = 1$. The small source size derived here ($2.3''$) is consistent with the size of the VyCN emission detected with BIMA by Liu and Snyder [26] (see their figure 2a) and with the similar fluxes detected by Friedel et al. [29] with BIMA and the NRAO 12 m telescope (only 10% of the 12 m flux is missed by BIMA). This source size is also similar to the one measured for aminoacetonitrile [16]. Therefore, the emission of VyCN and its ^{13}C isotopologues arises mainly from the two compact hot cores separated by about $5.3''$ in the North-South direction. These two hot cores are not spatially resolved with the IRAM 30m telescope but are clearly separated with interferometers like the PdBI and the ATCA. The main one with a velocity of 63 km s^{-1} corresponds to the so-called “Large Molecule Heimat” (LMH for short). The third velocity component, identified at 55 km s^{-1} , most likely corresponds to the blueshifted linewing detected with the PdBI in cyanoacetylene HC_3N (see Fig. 5m of [16]), and may be associated with an outflow.

We derived a column density of $8 \times 10^{17} \text{ cm}^{-2}$ for the main velocity component of VyCN which corresponds to the LMH (see Table 2). This value is a factor of 3-4 larger than the one calculated by Liu and Snyder [26], which is not surprising since they analyzed their spectrum of VyCN at 83.2 GHz assuming optically thin emission whereas our LTE modeling indicates an optical depth of ~ 2.3 for this transition in our survey. In addition, they may not have taken into account the contribution of the low-lying vibrational modes to the partition function as was done here (about 25%). The temperature derived from our LTE analysis (170 K) is in good agreement with the temperature measured by Ikeda et al. [28] for their VyCN transitions observed with the Nobeyama radiotelescope ($141 \pm 56 \text{ K}$). On the other hand, no evidence for a high-temperature component (440 K) was found for the main isotopologue in its ground vibrational state in the present survey in contrast to what was reported by Nummelin and Bergman [3]. Since the column densities of VyCN and its ^{13}C isotopologues have been independently measured here, the $^{12}\text{C}/^{13}\text{C}$ isotopic ratio of VyCN can be calculated from the column-density ratio. As a result, we find a $^{12}\text{C}/^{13}\text{C}$ isotopic ratio of 21 for VyCN , which is fully consistent with the standard value listed by Wilson and Rood for the Galactic Center [27].

With a mean H_2 column density of $N_{\text{H}_2} = 1.3 \times 10^{25} \text{ cm}^{-2}$ [16], a relative abundance of $\sim 6.2 \times 10^{-8}$ is derived for VyCN in the LMH, and $\sim 2.9 \times 10^{-9}$ for each of its ^{13}C isotopologues. The abundance of VyCN derived here is more than one order of magnitude larger than the abundances recently found by Fontani et al. in a sample of massive hot cores [30].

We also detect the ^{13}C isotopologues of ethyl cyanide ($\text{C}_2\text{H}_5\text{CN}$, EtCN for short) in our survey of Sgr B2(N). Rest frequencies were taken from the CDMS [21,22]; the entries were based on the laboratory data from Ref. [31]. The latter work also reports the detection of ^{13}C isotopologues of EtCN for the first time in space. The current LTE analysis of our Sgr B2(N) survey (Belloche et al., *in prep.*) shows that the detected lines are optically thin, with opacities smaller than 0.4. For the main velocity component of each ^{13}C isotopologue, a column density of $4 \times 10^{16} \text{ cm}^{-2}$ is found with a source size of $3''$ derived from the detected EtCN lines and a temperature of 170 K. In the LTE approximation, the contribution of the low-lying vibrational modes to the partition function is estimated to be about 40% at 170 K, which yields a total column density of $5.6 \times 10^{16} \text{ cm}^{-2}$ for the ^{13}C isotopologues of EtCN . Therefore, the column-density ratio of the ^{13}C isotopologues of VyCN to the ^{13}C isotopologues of EtCN is $R \approx 0.7$ in the LMH, which is in good agreement with what Liu and Snyder [26] found for the ^{12}C species. However, they may not trace the same material in this source since the VyCN emission looks single-peaked in interferometric maps while the EtCN emission is definitively double-peaked (see [26] and Fig. 5h of [16]). For the second velocity component corresponding to the northern hot core in Sgr B2(N), we find a column density of $5 \times 10^{16} \text{ cm}^{-2}$ for the ^{13}C isotopologues of EtCN with a source size of $2.3''$ and a temperature of 170 K. After correction for the contribution of the low-lying vibrational modes, the total column density is about $7 \times 10^{16} \text{ cm}^{-2}$. This gives a column-density ratio $R \approx 0.16$ for the northern hot core of Sgr B2(N).

In hot cores, EtCN is thought to evaporate from the dust grains where it was formed and to subsequently form VyCN through gas-phase reactions [30,32]. In the dynamical-chemical calculations of Caselli et al. [30,32] modeling the gas phase and surface chemistry in a collapsing core with a density of 10^7 cm^{-3} and a temperature of 200 K, the abundance ratio R of VyCN to EtCN increases initially with time as VyCN is progressively produced from EtCN , reaches a maximum of about 0.5, and then starts to decrease when the abundances of many complex molecules also drop. This ratio R may therefore be used as a chemical clock [30]. The ratio $R \approx 0.7$ found here for the LMH is even larger than the maximum predicted by the model. Fontani et al. [30] mentioned that the model may underestimate the production of VyCN (thus R too) due to a missing reaction of EtCN with H_3O^+ in the chemical network. If we take the large value found in LMH as the true maximum, then the age of the LMH is $\sim 8 \times 10^4 \text{ yr}$ since the beginning of the evaporation of the grain mantles in the framework of this model. On the other hand, the ratio R about 4 times smaller

found for the northern hot core suggests that it is at a different evolutionary stage than the LMH, either younger (3×10^4 yr) or older (1.6×10^5 yr), depending on whether it is before or after the peak of R . We note however that the H_2 density in the LMH is about $2 \times 10^8 \text{ cm}^{-3}$ [16], which is one order of magnitude larger than the density assumed by Caselli et al. [32] for their model. The chemical timescales may therefore be shorter in the LMH than in the model, and the ages determined above may be overestimated.

7 Conclusion

Very accurate transition frequencies have been obtained for five isotopic species of VyCN in their ground vibrational states within the millimeter-wave domain. The resulting spectroscopic parameters are accurate enough to identify the minor isotopic species in the interstellar medium or circumstellar envelopes up to about 700 GHz. This corresponds approximately with the foreseen upper frequency limit of ALMA of 720 GHz which may even be extended up to around 950 GHz later. On the other hand, none of the high frequency molecular line surveys of Orion KL carried out with comparatively large (~ 10 m) single dish telescopes covering the frequency regions 455 – 507 GHz [23], 607 – 725 GHz [24], and 795 – 903 GHz [25] revealed any features of the main isotopic species of VyCN while even vibrationally excited VyCN was observed in the 325 – 360 GHz survey [2]. Therefore, it is not clear at present if the minor isotopic species of VyCN will be observable with ALMA in its highest frequency bands; however the expected very high sensitivity and spatial resolution may make this fairly likely. Because of previous laboratory data [12], predictions for the main isotopic species should be reliable up to at least 1 THz. The current data significantly improve the predictions for the weaker lines. Extensive predictions of the rotational spectra will be available in the CDMS [21,22] for all these species. These predictions will be a contribution to minimize the so-called “weed problem”, that means that features of abundant molecules in space, such as VyCN , may prevent weaker features of desired molecules to be identified unambiguously unless sufficiently weak features of the more abundant species are known accurately enough. The “weed problem” is of particular concern for radiotelescope arrays such as the SMA or, even more so, for ALMA.

With the accurate transition frequencies obtained in the present work, we could identify for the first time in space the three ^{13}C species of VyCN in our 3 mm molecular line survey of the massive star forming region Sgr B2(N). The emission is detected in two compact ($\sim 2.3''$) hot cores with a temperature of 170 K, a column density of $\sim 3.8 \times 10^{16}$ and $1.1 \times 10^{16} \text{ cm}^{-2}$, and a velocity of 63 and 73 km s^{-1} , respectively. In the strongest source, the “Large Molecule Heimat” with a velocity of 63 km s^{-1} , a relative abundance of 2.9×10^{-9} has

been derived for each ^{13}C species of VyCN , and an isotopic ratio $^{12}\text{C}/^{13}\text{C}$ of 21 has been measured. Based on a comparison to the column densities measured for the ^{13}C species of ethyl cyanide also detected in this survey, it is suggested that the two hot cores of Sgr B2(N) are in different evolutionary stages.

8 Acknowledgments

H.S.P.M. is grateful for initial funding provided by the Deutsche Forschungsgemeinschaft (DFG) through the Sonderforschungsbereich (SFB) 494. Recently, he has been supported by the Bundesministerium für Bildung und Forschung (BMBF) administered through Deutsches Zentrum für Luft- und Raumfahrt (DLR). His support was aimed in particular at maintaining the CDMS. Further financial resources have been furnished by the Land Nordrhein-Westfalen.

References

- [1] F.F. Gardner, G. Winnewisser, *Astrophys. J.* 195 (1975) L127–L130.
- [2] P. Schilke, T.D. Groesbeck, G.A. Blake, T.G. Phillips, *Astrophys. J. Suppl. Ser.* 108 (1997) 301–337.
- [3] A. Nummelin, P. Bergman, *Astron. Astrophys.* 341 (1999) L59–L62.
- [4] H.E. Matthews, T.J. Sears, *Astrophys. J.* 272 (1983) 149–153.
- [5] M. Agúndez, J.P. Fonfría Expósito, J. Cernicharo, J.R. Pardo, M. Guélin, *Astron. Astrophys.* 479 (2008) 493–501.
- [6] W.S. Wilcox, J.H. Goldstein, J.W. Simmons, *J. Chem. Phys.* 22 (1954) 516–518.
- [7] C.C. Costain, B.P. Stoicheff, *J. Chem. Phys.* 30 (1959) 777–782.
- [8] M.C.L. Gerry, G. Winnewisser, *J. Mol. Spectrosc.* 48 (1973) 1–16.
- [9] J. Demaison, A. Bouchy, G. Roussy, J. Barriol, *Compt Rend.* 276C (1973) 967–969.
- [10] M. Stolze, D.H. Sutter, *Z. Naturforsch.* 40a (1985) 998–1010.
- [11] G. Cazzoli, Z. Kisiel *J. Mol. Spectrosc.* 130 (1988) 303–315.
- [12] J. Demaison, J. Cosléou, R. Bocquet, A.G. Lesarri *J. Mol. Spectrosc.* 167 (1996) 400–418.
- [13] O.I. Baskakov, S.F. Dyubko, V.V. Ilyushin, M.N. Efimenko, V.A. Efremov, S.V. Podnos, E.A. Alekseev, *J. Mol. Spectrosc.* 179 (1996) 94–98.

- [14] J.M. Colmont, G. Wlodarczak, D. Priem, H.S.P. Müller, E.H. Tien, R.J. Richards, M.C.L. Gerry, J. Mol. Spectrosc. 181 (1997) 330–344.
- [15] S. Thorwirth, H.S.P. Müller, H. Lichau, G. Winnewisser, G.C. Mellau, J. Mol. Struct. 695–696 (2004) 263–267.
- [16] A. Belloche, K.M. Menten, C. Comito, H.S.P. Müller, P. Schilke, J. Ott, S. Thorwirth, C. Hieret, Astron. Astrophys. (2008), *in press*.
- [17] G. Winnewisser, A.F. Krupnov, M.Y. Tret'yakov, M. Liedtke, F. Lewen, A.H. Saleck, R. Schieder, A.P. Shkaev, S.V. Volokhov, J. Mol. Spectrosc. 165 (1994) 294–300.
- [18] H.S.P. Müller, S. Brünken J. Mol. Spectrosc. 232 (2005) 213–222.
- [19] H.S.P. Müller, M.C. McCarthy, L. Bizzocchi, H. Gupta, S. Esser, H. Lichau, M. Caris, F. Lewen, J. Hahn, C. Degli Esposti, S. Schlemmer, P. Thaddeus, Phys. Chem. Chem. Phys. 9 (2007) 1579–1586.
- [20] H.M. Pickett, J. Mol. Spectrosc. 148 (1991) 371–377.
- [21] H.S.P. Müller, S. Thorwirth, D.A. Roth, G. Winnewisser, Astron. Astrophys. 370 (2001) L49–L52.
- [22] H.S.P. Müller, F. Schlöder, J. Stutzki, G. Winnewisser, J. Mol. Struct. 742 (2005) 215–227.
- [23] G.J. White, M. Araki, J.S. Greaves, M. Ohishi, N.S. Higginbottom, Astron. Astrophys. 407 (2003) 589–607.
- [24] P. Schilke, D.J. Benford, T.R. Hunter, D.C. Lis, T.G. Phillips, Astrophys. J. Suppl. Ser. 132 (2001) 281–364.
- [25] C. Comito, P. Schilke, T.G. Phillips, D.C. Lis, F. Motte, D. Mehringer, Astrophys. J. Suppl. Ser. 156 (2005) 127–167.
- [26] S. Liu, L.E. Snyder, Astrophys. J. 523 (1999) 683–689.
- [27] T.L. Wilson, R.T. Rood, Ann. Rev. Astron. Astrophys. 32 (1994) 191–226.
- [28] M. Ikeda, M. Ohishi, A. Nummelin, J.E. Dickens, P. Bergman, Å. Hjalmarson, W. M. Irvine, Astrophys. J. 560 (2001) 792–805.
- [29] D.N. Friedel, L. E. Snyder, B. E. Turner, A. Remijan, Astrophys. J. 600 (2004) 234–253.
- [30] F. Fontani, I. Pascucci, P. Caselli, F. Wyrowski, R. Cesaroni, C. M. Walmsley, Astron. Astrophys. 470 (2007) 639–652.
- [31] K. Demyk, H. Mäder, B. Tercero, J. Cernicharo, J. Demaison, L. Margulès, M. Wegner, S. Keipert, M. Sheng, Astron. Astrophys. 466 (2007) 255–259.
- [32] P. Caselli, T.I. Hasegawa, E. Herbst, Astrophys. J. 408 (1993) 548–558.

Table 1
Spectroscopic parameters^a (MHz) of isotopic species of vinyl cyanide.

Parameter	H ₂ CCHCN	H ₂ ¹³ CCHCN	H ₂ C ¹³ CHCN	H ₂ CCH ¹³ CN	H ₂ CCHC ¹⁵ N
<i>A</i>	49850.69674 (20)	49195.292 (89)	48639.693 (31)	49799.643 (26)	49655.880 (173)
<i>B</i>	4971.163651 (24)	4837.58023 (12)	4948.98019 (13)	4948.36515 (12)	4819.66825 (18)
<i>C</i>	4513.877260 (25)	4398.24203 (12)	4485.38246 (13)	4494.65445 (13)	4387.04599 (17)
<i>D_K</i> × 10 ³	2714.880 (19)	2710.8 (163)	2597.1 (59)	2630.3 (64)	2762. (35)
<i>D_{JK}</i> × 10 ³	−85.01578 (79)	−86.3393 (51)	−79.9149 (30)	−85.4947 (32)	−82.6057 (48)
<i>D_J</i> × 10 ³	2.182401 (32)	2.11922 (12)	2.11940 (9)	2.16156 (10)	2.04954 (20)
<i>d₁</i> × 10 ⁶	−456.5241 (90)	−438.491 (112)	−453.328 (123)	−451.389 (150)	−420.381 (174)
<i>d₂</i> × 10 ⁶	−30.8801 (42)	−28.023 (42)	−31.835 (32)	−29.678 (41)	−28.361 (78)
<i>H_K</i> × 10 ⁶	384.14 (45)	384.	364.	370.	384.
<i>H_{KJ}</i> × 10 ⁶	−6.9401 (81)	−7.037 (35)	−6.785 (18)	−6.766 (23)	−6.931 (51)
<i>H_{JK}</i> × 10 ⁶	−0.28487 (27)	−0.2835 (37)	−0.2607 (16)	−0.2912 (19)	−0.2633 (34)
<i>H_J</i> × 10 ⁹	5.7252 (92)	5.539 (42)	5.381 (49)	5.612 (66)	5.073 (67)
<i>h₁</i> × 10 ¹²	2276.3 (53)	2243. (46)	2436. (64)	2181. (88)	1946. (77)
<i>h₂</i> × 10 ¹²	367.8 (38)	330.2	375.6	360.0	319.2
<i>h₃</i> × 10 ¹²	89.15 (83)	79.1	92.9	87.1	75.5
<i>L_K</i> × 10 ⁹	−57.4 (33)	−58.	−54.7	−55.5	−58.0
<i>L_{KKJ}</i> × 10 ⁹	1.213 (24)	1.195 (17)	1.221 (27)	1.197 (45)	1.367 (108)
<i>L_{JK}</i> × 10 ¹²	−81.6 (25)	−57.1 (252)	−76.9 (65)	−82.5 (79)	−81.9 (269)
<i>L_{JJK}</i> × 10 ¹²	1.785 (37)	1.63	1.71	1.76	1.63
<i>L_J</i> × 10 ¹⁵	−21.65 (85)	−19.1	−20.8	−21.3	−18.9
<i>l₁</i> × 10 ¹⁵	−8.89 (103)	−7.85	−8.94	−8.77	−7.75
<i>l₂</i> × 10 ¹⁵	−3.78 (99)	−3.23	−3.75	−3.60	−3.11
<i>l₃</i> × 10 ¹⁵	−1.42 (38)	−1.25	−1.50	−1.41	−1.19
<i>l₄</i> × 10 ¹⁵	−0.223 (50)	−0.186	−0.230	−0.211	−0.174
<i>P_{KKKJ}</i> × 10 ¹⁵	−227. (32)	−210.	−202.	−225.	−218.
<i>P_{KKJ}</i> × 10 ¹⁵	−108.9 (52)	−99.	−99.	−107.	−102.
<i>S_{KKKKJ}</i> × 10 ¹⁸	157. (17)	144.	136.	155.	150.
<i>χ_{aa}</i>	−3.78907 (40)	−3.76634 (55)	−3.80158 (55)	−3.78580 (40)	n. a.
<i>χ_{bb}</i>	1.68606 (43)	1.6547 (41)	1.6902 (41)	1.68435 (167)	n. a.
<i>χ_{cc}</i>	2.10301 (49)	2.1116 (40)	2.1114 (40)	2.10145 (166)	n. a.
<i>C_{aa}</i> × 10 ³	2.20 (30)	2.20	2.20	2.20	—
<i>C_{bb}</i> × 10 ³	0.78 (17)	0.78	0.78	0.78	—
<i>C_{cc}</i> × 10 ³	1.43 (17)	1.43	1.43	1.43	—

^a Numbers in parentheses are one standard deviation in units of the least significant figures. Parameter values with no uncertainties given were estimated from those of the main isotopic species and kept fixed; see section 3. A long dash indicates parameters that are determinable in theory, but have not been determined here; n. a. stands for not applicable.

Table 2

Parameters of our best-fit LTE model of vinyl cyanide (VyCN) and its ^{13}C isotopologues. We used the same parameters for all three ^{13}C isotopologues. For each species, each line corresponds to a different velocity component in Sgr B2(N).

Molecule	Size ^a	T _{rot}	N ^b	FWHM	V _{off} ^c
	($''$)	(K)	(cm^{-2})	(km s^{-1})	(km s^{-1})
(1)	(2)	(3)	(4)	(5)	(6)
VyCN	2.3	170	8.00×10^{17}	7.0	-1.0
	2.3	170	2.40×10^{17}	7.0	9.0
	2.3	170	1.00×10^{17}	10.0	-9.0
$^{13}\text{VyCN}$	2.3	170	3.75×10^{16}	7.0	-1.0
	2.3	170	1.13×10^{16}	7.0	9.0
	2.3	170	0.47×10^{16}	10.0	-9.0

(a) Source diameter (FWHM).

(b) The column densities listed here for all isotopic species of VyCN were computed with partition functions that take into account contributions from the low-lying vibrational modes which amount to about 25% in the LTE approximation at 170 K.

(c) Velocity offset with respect to the systemic velocity of Sgr B2(N) $V_{\text{lsr}} = 64 \text{ km s}^{-1}$.

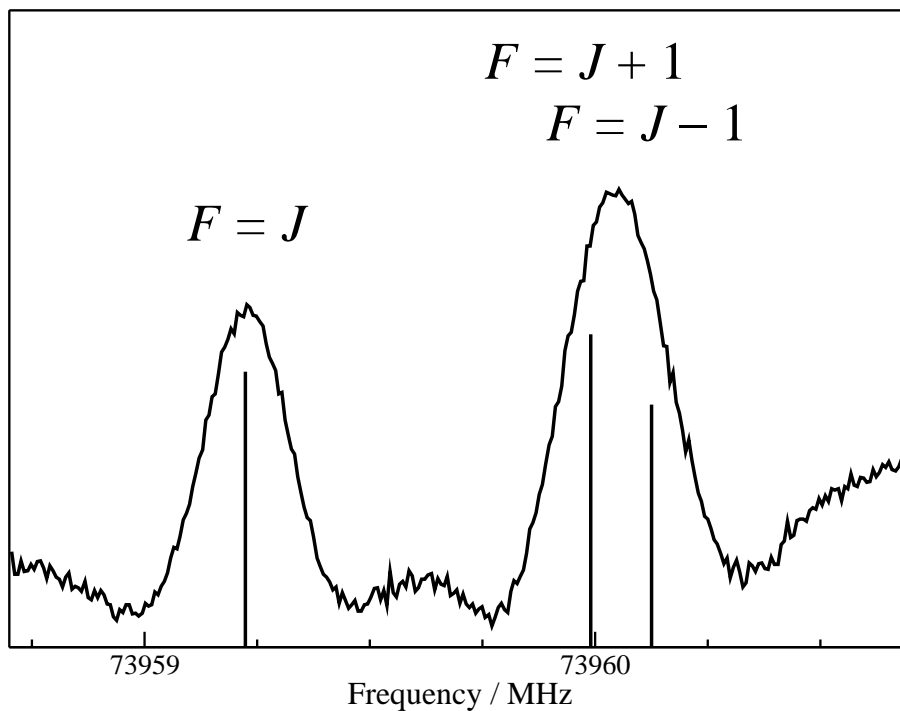


Fig. 1. Portion of the rotational spectrum of vinyl cyanide in the region of the prolate paired $J_{K_a, K_c} = 8_{7,1} - 7_{7,0}$ & $8_{7,2} - 7_{7,1}$ transition of $\text{H}_2^{13}\text{C}=\text{CH}-\text{C}\equiv\text{N}$ demonstrating the partially resolved ^{14}N hyperfine splitting. The calculated positions and relative intensities of the individual hyperfine components are indicated by vertical lines.

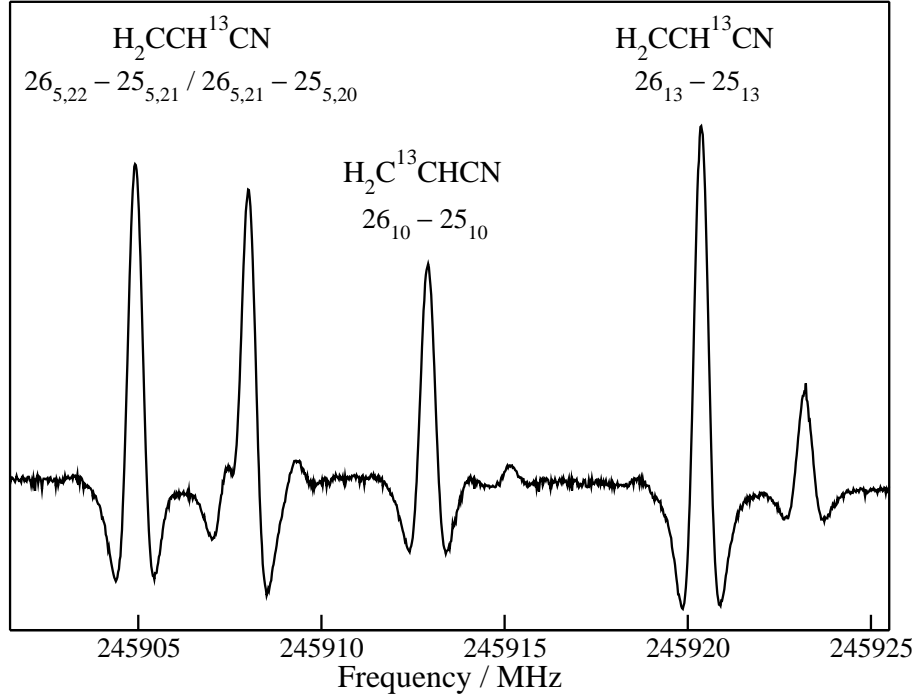


Fig. 2. Portion of the rotational spectrum of vinyl cyanide in the region of the $J = 26 - 25$ a -type R -branch transitions of $\text{H}_2\text{C}=\text{CH}-^{13}\text{C}\equiv\text{N}$ and $\text{H}_2\text{C}=^{13}\text{CH}-\text{C}\equiv\text{N}$. The stronger features in this recording can be assigned to these two isotopic species. Since $K_a + K_c = J$ or $J + 1$, K_c has been omitted for the prolate paired transitions having $K_a = 10$ and 13 , respectively. The weaker features can not be assigned at present. As one can see, two weaker lines affect the position of the $26_{5,21} - 25_{5,20}$ transition of $\text{H}_2\text{C}=\text{CH}-^{13}\text{C}\equiv\text{N}$.

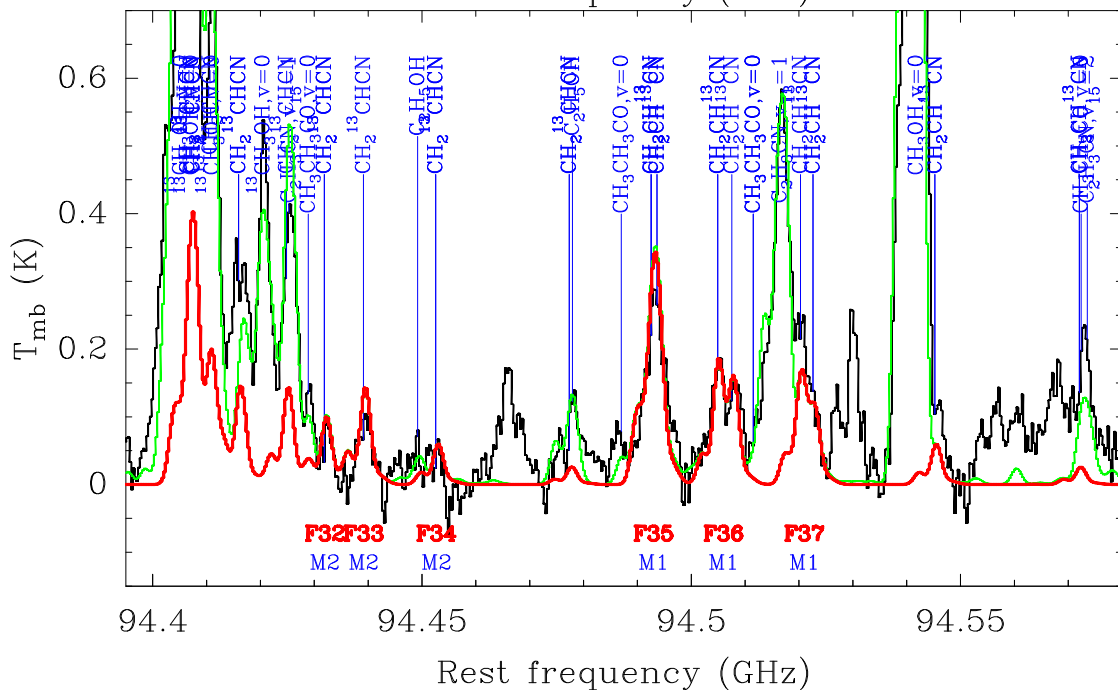


Fig. 3. Selected transitions of the ^{13}C isotopologues of vinyl cyanide detected with the IRAM 30m telescope. In each panel, the spectrum observed toward Sgr B2(N) is shown in black, while the LTE synthetic spectrum including the three ^{13}C isotopologues of vinyl cyanide is overlaid in red and the LTE model including all identified molecules in green. The detected features are labeled in red, as listed in Col. 9 of Table S2 in the supplementary material. The identified lines are labeled in blue (M1, M2, and M3 stand for the three ^{13}C isotopologues as in Col. 2 of Table S2). All observed lines which have no counterpart in the green spectrum are still unidentified. The systemic velocity assumed for Sgr B2(N) is 64 km s^{-1} .